Journal of Inorganic Biochemistry 123 (2013) 23–33

Contents lists available at SciVerse ScienceDirect

Journal of Inorganic Biochemistry

journal homepage: www.elsevier.com/locate/jinorgbio

Improvement of the antihypertensive capacity of candesartan and trityl candesartan by their SOD mimetic copper(II) complexes

María S. Islas [a], Teófilo Rojo [b], Luis Lezama [b], Mercedes Griera Merino [c], María A. Cortes [c], Manuel Rodriguez Puyol [c], Evelina G. Ferrer [a], Patricia A.M. Williams [a,*]

[a] Centro de Química Inorgánica (CEQUINOR/CONICET/UNLP)-Facultad de Ciencias Exactas, Universidad Nacional de La Plata, 47 esq 115, 1900 La Plata, Argentina
[b] Departamento de Química Inorgánica, Facultad de Ciencia y Tecnología, Universidad del País Vasco, Apdo 644, 48080 Bilbao, Spain
[c] Departamento de Fisiología, Universidad de Alcalá, Campus Universitario, 28871-Alcalá de Henares, Madrid, Spain

ARTICLE INFO

Article history:
Received 16 November 2012
Received in revised form 13 February 2013
Accepted 13 February 2013
Available online 21 February 2013

Keywords:
Antihypertensive drugs
Candesartan
Copper complexes
Antioxidants
Human mesangial contractile cells

ABSTRACT

Two new complexes $[Cu(Cand)(H_2O)_4]$ **[1]** and $[Cu_2(TCand)_4(H_2O)_2]\cdot 4H_2O$ **[2]** (Cand = candesartan; TCand = trityl candesartan) have been synthesized and thoroughly characterized. The FTIR, Raman, EPR and diffuse reflectance spectra of the solid compounds show a dimeric complex for **[2]** with carboxylate bridging of the type found in copper(II) acetate. Both elemental analysis and thermal measurements allow the determination of the total stoichiometries of both complexes. The stability measurements show that the compounds are stable in ethanolic solutions at least for 1 h, while the preservation of the overall stochiometry for both species in solution has been determined by spectrophotometric titrations. By metal complexation the absence of antioxidant behavior of both sartans has been improved. Complexes **[1]** and **[2]** are strong superoxidedismutase mimetic compounds and complex **[2]** also behaves as a peroxyl radical scavenger. Furthermore, this higher antioxidant activity works in parallel with the improvement of the expansive activity over the angiotensin II-induced contracted human mesangial cells. These new complexes exhibit even higher efficiency as drugs in comparison with the free non-complexed medication with increased antioxidant ability expressing higher capacity to block the angiotensin II contractile effect. This study provides a new insight into the development of copper(II) complexes as potential drugs.

1. Introduction

Treatment of hypertension involves several different classes of drugs. Sartans are synthetic substances that have the renin–angiotensin system (RAS) as the target of their mechanism of action. They inhibit the angiotensin converting enzyme (ACE) which is mainly responsible for the conversion of angiotensin I into angiotensin II (that induces a direct vasoconstrictor action causing hypertension) [1].

Candesartan belongs to the class of AT2 receptor antagonists (AT2 blockers) and is used to treat high blood pressure but it is poorly absorbed when administered orally. Therefore, the prodrug candesartan cilexetil was developed. The prodrug undergoes rapid and complete ester hydrolysis in the intestinal wall and converted to candesartan, its active metabolite, during absorption from the gastrointestinal tract [2,3].

New therapeutical anticancer strategies proposing administration of candesartan were developed since the knowledge that angiotensin II acts as an angiogenic factor and the hypothesis that it is involved in regulation of tumor angiogenesis in cancer. Candesartan was found able for targeting tumor angiogenesis by inhibition of AT1R (angiotensin I receptor) in different kinds of cancer [4–9]. Candesartan can also attenuate induced oxidative stress and NAD(P)H oxidase activity [10]. However, it has been suggested that its antioxidant effect is independent of AT1R blockade [11].

In general, most of the sartans are composed of an appropriately substituted heterocyclic nucleus coupled to an acidic group (carboxylic or tetrazole) bearing biphenyl system through a methylene linker. In particular, candesartan has the benzimidazole group substituted with carboxyl function at the 7-position [2].

Modifications of the structure of candesartan were performed in order to improve the biological effect of the sartan. It has been demonstrated that methylation of the tetrazole ring with the concomitant loss of the acidic group produced a reduction of the potency of the drug in 1000 units of magnitude. From these data it was concluded that an ionic interaction to the receptor is more probable than H bonding interactions [12]. In order to test these observations we have also included trityl candesartan (HTCand) to perform comparisons with the behavior of candesartan (H_2Cand) (see Fig. 1).

Other structural modifications of sartans including the formation of novel molecules between losartan and compounds with antioxidant activities that produced both antihypertensive and cytoprotective effects, [13] and the so-called NO-sartans that merge both antihypertensive

* Corresponding author at: Centro de Química Inorgánica (CEQUINOR/CONICET,UNLP), Facultad de Ciencias Exactas, Universidad Nacional de La Plata, 47 esq 115, 1900 La Plata, Argentina. Fax: +54 2214259485.
E-mail address: williams@quimica.unlp.edu.ar (P.A.M. Williams).

0162-0134/$ – see front matter © 2013 Elsevier Inc. All rights reserved.
http://dx.doi.org/10.1016/j.jinorgbio.2013.02.005

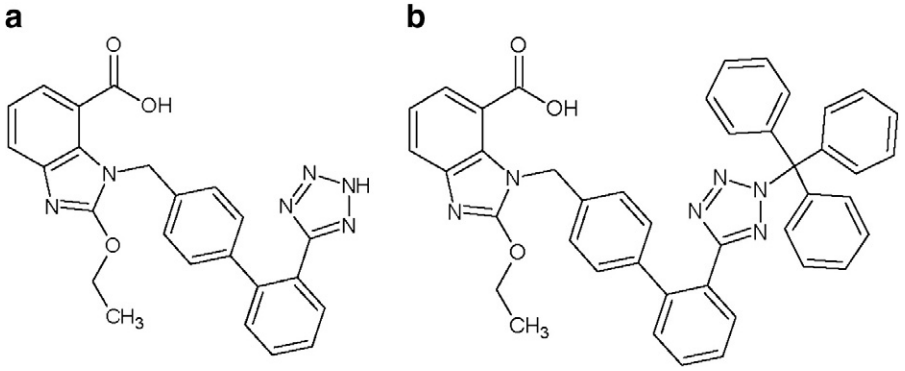

Fig. 1. a) candesartan (H_2Cand); b) trityl candesartan (HTCand).

properties using nitric oxide-releasing drugs and AT1 antagonists have been reported. These pharmacodynamic hybrids improved the action of the "native" sartans [14,15]. Taking into account that these modifications strengthen the action of the drugs, we have, therefore, undertaken the design of another class of hybrids by synthesizing coordination compounds with the biometal copper(II) and both candesartan and trityl candesartan. Metal complexes have been widely applied in clinics for centuries and the great successes achieved with platinum-based antitumor agents have promoted the development of metal-based drugs. Particularly, copper is an essential element involved in several biological functions. All tissues of the body need it for normal metabolic functions. It is able to reduce inflammations, strengthen connective tissue, restore hair color and the oxidative energy metabolism as well as fight parasites and cancer. It has been observed that the serum level of copper is often elevated in animals and humans with cancer with an associated decrease in the concentration of the antioxidant copper-dependent enzymes [16]. Besides, the role of copper in maintaining cardiovascular health has been well established. Copper is essential both for its role in antioxidant enzymes, like Cu–Zn superoxidedismutase and ceruloplasmin, as well as its role in lysyl oxidase, essential for the strength and integrity of the heart and blood vessels. Copper deficiency has produced many of the same abnormalities present in cardiovascular disease [17].

We have previously described the effects of two analog copper(II) complexes with losartan and valsartan and determined that upon complexation the antioxidant activities (tested for losartan–copper compound) and the inhibitory effects on the tumoral cell line proliferation were improved [18,19]. In the present communication we describe the preparation and structural characterization of two new copper(II) complexes with candesartan and trityl candesartan and determine their antioxidant behavior and the ability of AT2 to reduce planar cell surface area in cells pretreated with these new compounds in comparison with free copper(II) ion and the free ligands.

2. Materials and methods

2.1. Reagents and instrumentation

All chemicals were of analytical grade and used without further purification. Copper(II) chloride dihydrate was purchased from Riedel de Häen, pure commercial samples of candesartan and trityl candesartan (Hangzhou Garden Trading Co., Ltd (China)) were used as supplied. FTIR spectra of powdered samples (as pressed KBr pellets) were measured with a Bruker IFS 66 FTIR-spectrophotometer from 4000 to 400 cm^{-1}. A total of 60 scans were accumulated. Spectral resolution was ± 4 cm^{-1}. FT-Raman spectra were measured using the FRA 106 Raman accessory. A continuous-wave Nd:YAG laser working at 1064 nm was employed for Raman excitation. A germanium detector operating at liquid nitrogen temperature was used. Raman scattering radiation was collected with a standard spectral resolution of ± 4 cm^{-1}. Electronic absorption spectra were recorded on a Hewlett-Packard 8453 diode-array spectrophotometer, using 1 cm quartz cells. Diffuse reflectance spectra were registered with a Shimadzu UV-300 instrument, using MgO as an internal standard. Elemental analyses (EA) for carbon, hydrogen and nitrogen were performed using a Carlo Erba EA 1108 analyzer. Thermogravimetric analysis (TG) and differential thermal analysis (DTA) were performed with Shimadzu systems (models TG-50 and DTA-50, respectively), working in an oxygen flow of 50 mL/min and at a heating rate of 10 °C/min. Sample quantities ranged between 10 and 20 mg. Al_2O_3 was used as a differential thermal analysis standard. A Bruker ESP300 spectrometer operating at the X-band and equipped with standard Oxford Instruments low-temperature devices (ESR900/ITC4) was used to record the EPR spectrum of the complex at room temperature in the solid state. A computer simulation of the EPR spectra was performed using the program SimFonia [20].

2.2. Preparative

[Cu(Cand)(H_2O)$_4$] (CuCand) **[1]**: A solution of $CuCl_2 \cdot 2H_2O$ in ethanol (1 mmol, 5 mL) was added under continuous stirring to an ethanolic solution of candesartan (1 mmol, 10 mL). The solution was allowed to stir at 60 °C and an aqueous solution of 1 M NaOH was added up to pH 7–8. When the final volume of the solution was reduced by 80% a green precipitate was generated after water (5 mL) addition. The resulting solid product was filtered off, washed several times with water and dried in an oven at 60 °C. Anal. Calc.%: C, 50.2; H, 4.5; N, 14.6. Exp.%: C, 49.9; H, 4.4; N, 14.2. Thermogravimetric analysis confirmed the presence of two labile water molecules (Exp. loss: 6.4%. Calc. loss: 6.3%; endothermic peak, DTA, T<100 °C) and two additional water molecules were lost at higher temperature probably due to the stronger covalent bonds generated by the Jahn–Teller effect (Exp. loss: 6.5%. Calc. loss: 6.3%; endothermic peak, DTA, 100 °C<T<200 °C). At 800 °C the weight loss (86.1%, calc.; 86.0%, exp.) represents the formation of CuO that was characterized by FTIR spectroscopy. UV–visible spectrum (ethanol): 670 nm ($\varepsilon = 100.2$ M^{-1} cm^{-1}). Diffuse reflectance spectrum: 440 nm, 770 nm.

[Cu_2(TCand)$_4$(H_2O)$_2$]$\cdot 4H_2O$ (CuTCand) **[2]**: To an ethanolic solution of trityl candesartan (1 mmol) heated at 70 °C an ethanolic $CuCl_2 \cdot 2H_2O$ solution (0.5 mmol) was added under constant stirring. The pH value of the mixture was raised to 7 by addition of an aqueous 1 M NaOH solution. Then, the mixture was concentrated by evaporation until a final volume of 5 mL was attained. The addition of water (10 mL) gave a green solid that was filtered off, washed with water and dried in an oven at 60 °C. Anal. Calc.%: C, 69.7; H, 4.9; N, 11.3 Exp%: C, 70.0; H, 4.8; N, 11.2. By thermogravimetric analysis (TGA) it was determined that the four crystallization water molecules are lost at 80 °C with an endothermic DTA signal (weight loss, 2.4%)

and the two coordinated water molecules are lost at 140 °C (weight loss, 1.2%). The total experimental weight loss of 3.6% is in good agreement with the calculated value (3.6%). The final residue (CuO), characterized by FTIR spectroscopy was achieved at 800 °C. A good correlation was found for the experimental total weight loss of $\Delta\omega_{exp} = 86.8\%$ and the calculated value, $\Delta\omega_{calcd} = 86.9\%$. UV–visible spectrum (ethanol): 690 nm ($\varepsilon = 202.6\ M^{-1}\ cm^{-1}$). Diffuse reflectance spectrum: 400 nm, 750 nm.

2.3. Spectrophotometric titrations

In order to establish the stoichiometry of the complexes in solution the molar ratio method was applied. The absorption spectra of different ethanolic solutions of 0.025 M candesartan or trityl candesartan with or without $CuCl_2 \cdot 2H_2O$ were measured. In both cases ligand-to-metal molar ratios from 10 to 0.75 were used and the pH values were adjusted to 8.4 (candesartan) and 7 (trityl candesartan) with a 0.1 M NaOH solution.

2.4. Antioxidant properties

In these experiments the sartans and the copper complexes were dissolved in the minimum quantity of 96% ethanol in order to avoid precipitations, and then they were added to the aqueous buffer and the substrate solutions. The same quantity of ethanol was added to the solutions for the basal state measurements in each case. The concentration of ethanol in each test was different but achieved a maximum of 5% in the final reaction mixtures.

2.4.1. 1,1-Diphenyl-2-picrylhydrazyl assay

The antiradical activity of sartans and the copper complexes was measured in triplicate using a modified Yamaguchi et al. [21] method. A methanolic solution of 1,1-diphenyl-2-picrylhydrazyl radical ($DPPH^{\cdot}$) (4 mL, 40 ppm) was added to 1 mL of the antioxidant solutions in 0.1 M tris(hydroxymethyl)aminomethane–HCl buffer (pH 7.1) at 25 °C, giving final concentrations from 10 to 500 μM. From the UV–visible (UV–vis) spectra, the absorbance at 517 nm was measured after 60 min of the reaction in the dark and compared with the absorbance of control prepared in a similar way without the addition of the antioxidants (this value was assigned arbitrarily as 100).

2.4.2. 2,2′-Azinobis(3-ethylbenzothiazoline-6-sulfonic acid) diammonium salt decoloration assay

The total antioxidant activity was measured using the Trolox (6-hydroxy-2,5,7,8-tetramethylchroman-2-carboxylic acid) equivalent antioxidant coefficient (TEAC). The radical cation of 2,2′-azinobis(3-ethylbenzothiazoline-6-sulfonic acid) diammonium salt (ABTS) was generated by incubating ABTS with potassium persulfate. Chemical compounds that inhibit the potassium persulfate activity may reduce the production of $ABTS^{\cdot+}$. This reduction resulted in a decrease of the total $ABTS^{\cdot+}$ concentration in the system and contributed to the total $ABTS^{\cdot+}$ scavenging capacity. Briefly, an aqueous solution of ABTS (0.25 mM) and potassium persulfate (0.04 mM) was incubated in the dark for 24 h. The solution was prepared in 0.1 M KH_2PO_4–NaOH buffer (pH 7.4). To 990 μL of this mixture, 10 μL of the sartans, the complexes, or the Trolox standard in phosphate buffer was added (final concentrations 0–100 μM). The reduction of $ABTS^{\cdot+}$ was monitored spectrophotometrically 6 min after the initial mixing at 25 °C. The percentage decrease of the absorbance of the band at 734 nm was calculated considering that the basal condition (without antioxidant additions) had been assigned as 100% and it was plotted as a function of the concentration of the samples giving the total antioxidant activity. The TEAC value was calculated from the slope of the plot of the percentage inhibition of absorbance versus the concentration of the antioxidant divided by the slope of the plot for Trolox [22,23].

2.4.3. Inhibition of peroxyl radical

Peroxyl radicals were generated by the thermal decomposition of 2,2-azobis(2-amidinopropane) dihydrochloride (AAPH). AAPH was chosen due to its ability to generate free radicals at a steady rate for extended periods of time (half life of 175 h). During the inhibition of the radicals pyranine (50 μM) was consumed and it was followed spectrophotometrically by the decrease in absorbance at 454 nm with a thermostated cell at 37 °C. The reaction solutions contained AAPH (50 mM) and pyranine (50 μM) in PBS (phosphate buffered saline) and several concentrations of the tested compounds dissolved in a mixture of ethanol–buffer (the concentration of ethanol in the final reaction mixture was 3%). The delay of pyranine consumption (lag phase) was calculated as the time before consumption of pyranine and compared with the effect of the different added compounds [24].

2.4.4. Superoxide dismutase assay

The superoxide dismutase (SOD) activity was examined indirectly using the nitroblue tetrazolium (NBT) assay. The indirect determination of the activity of sartans and the complexes was assayed by their ability to inhibit the reduction of NBT by the superoxide anion generated by the phenazine methosulfate and reduced nicotinamide adenine dinucleotide system. As the reaction proceeded, the formazan color developed and a change from yellow to blue was observed which was associated with an increase of the intensity of the band at 560 nm in the absorption spectrum. The system contained 0.5 mL of the sample, 0.5 mL of 1.40 mM reduced nicotinamide adenine dinucleotide, and 0.5 mL of 300 μM NBT, in 0.1 M KH_2PO_4–NaOH buffer (pH 7.4). After incubation at 25 °C for 15 min, the reaction was started by adding 0.5 mL of 120 μM phenazine methosulfate [25]. Then, the reaction mixture was incubated for 5 min. Each experiment was performed in triplicate and at least three independent experiments were performed in each case. The amount of complex (or ligand) that gave a 50% inhibition (IC_{50}) was obtained by plotting the percentage of inhibition versus the log of the concentration of the solution tested.

2.5. Determination of changes in planar cell surface area (PCSA)

The human mesangial cells (HMC) were plated in 20-mm plates, and studies were performed before they reached confluence. Cells were pretreated with different compounds (see figure legend) and then treated successively with angiotensin II. The cells were observed under phase contrast with an inverted PFX model TMS-F photomicroscope (magnification, 100×). Photographs of cells were taken a 0 min and after the 30 min with angiotensin II treatment. Every cell with a sharp margin suitable for the planimetric analysis was considered, and 6 to 12 cells were analyzed per photograph. PCSA was determined by computer-aided planimetric techniques. Measurements were performed by three different researchers in a blind fashion.

3. Results and discussion

3.1. Vibrational spectroscopy

The vibrational pattern of candesartan and its sodium salt was previously studied by density functional B3LYP method with the 6–31 + G(d,p) basis set [26]. Both FTIR and Raman spectra were compared with those of the copper candesartan complex. The experimental wavenumbers and the tentative assignments can be observed in Table 1.

The typical candesartan modes belonging to the NH group shifted, disappeared or reduced its intensity upon deprotonation and/or coordination (1479 cm^{-1}, 1238 cm^{-1} and 1134 cm^{-1}). The infrared spectrum of the sodium salt also differs somewhat from that of the complex with shifts of ca. 5–10 cm^{-1} in those bands due to the coordination of copper to the deprotonated nitrogen center. The other bands related to

Table 1
Assignment of the main bands of the FTIR and Raman spectra of protonated candesartan (H_2Cand), candesartan sodium salt (Na_2Cand), and the copper complex (CuCand) (band positions in cm^{-1}).

Assignment	H_2Cand		CuCand		Na_2Cand	
	FTIR	Raman	FTIR	Raman	FTIR	Raman
υ C=O + δ COH	1705 vs	1710 m	1703 w		1698 w	
υ C=C + υ C=N_{Bz} + ***$υ_{as}$ COO$^-$***			1649 sh		1647 sh	
υ C=C + υ C=N_{Bz}	1610 m	1613 vs 1608 sh	1617 m	1613 vs	1616 m	1613 vs
				1605 sh		1608 sh
						1605 vs
δ $_{ip}$ NNH $_{tz}$ + $δ_{ip}$ CCH $_{arom}$ + υ C=C	1549 vs	1552 m	1548 vs	1540 m	1546 vs	1548 w
δ $_{ip}$ CCH $_{arom}$ + scissor CH_2 + def CH_3 + ***υ C–C $_{tz\text{-}biph}$***	1517 sh	1519 w	1516 sh	1524 m	1525 sh	1524 m
						1509 m
δ NNH + υ C–$C_{tz\text{-}biph}$ + $δ_{ip}$ CCH_{arom}	1479 s	1487 w	1484 m		1489 m	1486 vw
δ NNH + δ CCH ip + scissor CH_2 + **δ COH** + υ CN_{Bz}	1461 sh	1454 w	1463 m	1456 w	1463 m	1461 w
υ C=$N_{Bz,\ tz}$ + $δ_{ip}$$CCH_{Bz}$ + ω CH_2 + τ CH_2 + **δ COH**	1426 s	1422 w	1426 m	1427 m	1426 m	1426 m
			1408 m	1415 s	1406 sh	
δs CH_3 + ω CH_2 + υ CN_{Bz} + ***υ C–COO$^-$***	1387 m	1372 w	1384 s		1389 s	1391 vw
δ NNH + ω CH_2 + υ C=C + υ CN_{Bz} + ***$υ_s$ COO$^-$***	1353 m	1355 sh	1352 m	1357 w	1354 m	1360 sh
δ COH + τ CH_2 + δ CCH + δ NCH + υ CN_{Bz}		1260 s		1278 m		1260 w
υ NN + **υ NH + δ NNH**	1238 vs	1226 m	1252 w	1253 m	1244 w	1245 m
				1226 w		1226 w
***υ* CO (COH)** + υ NN + δ CCH_{arom}	1212 sh	1187 m		1200 vw	1211 sh	1210 w
	1190 sh			1182 vw		1185 w
$δ_{ip\ arom}$ CCH + ρ CH_2 + ω CH_2 + **$δ_{ip}$ NNH** + υ CN_{Bz} + ***υ (Bz)C–C(COO$^-$)***	1134 m 1112 sh	1139 w 1119 w	1151 m	1152 w	1141 m	1148 m
			1114 w	1117 w	1109 w	1112 w
δ NNN + δ NCN + $δ_{op}$ CCH + ***υ (Bz)C–C(COO$^-$)***	1039 s	1013 m	1040 s	1012 s	1040 s	1012 s
	1002 sh		1009 w		1009 w	
$δ_{op}$ COH + $δ_{op}$ CCH_{Bz} + δ CCC (Et) + ***π CCOO (COO$^-$)***	823 m	814 s	849 m	825 w	849 m	812 m
			820 w		820 w	
$γ_{op}$ NH + $δ_{op}$ CCH + $δ_{ip}$$CCC_{arom}$ + ***π NNCC***	754 s	773 w	786 m	789 w	787 m	787 m
			763 s	751 vw	760 s	760 w
δ OCO (COOH) + δ (Bz)COC (Et)	698 m	702 w	697 vw		694 w	
π NNNH + Biph breath	674 sh	668 w				
Biph breath			670 w	685 vw	666 w	669 w

Bold: main modes of H_2Cand. Bold *italics*: main modes of Na_2Cand and CuCand.
Abbreviations: vs, very strong; s, strong; m, medium; w, weak; vw: very weak; sh, shoulder. ν, stretching; δ, bending; ω, wagging; τ, twisting; ρ, rocking; π, out of plane deformation (4 atoms); s, symmetric; as, antisymmetric; arom, aromatic; op, out of plane; ip, in plane.
Bz, benzimidazole; biph, biphenyl; tz, tetrazole; breath, breathing.

the NHtz modes that are associated with the stretching C=C and symmetric COO– modes (ca. 1550 cm^{-1} and 1350 cm^{-1}) [26] do not change upon deprotonation or coordination due to the strong intensities of the latter modes.

The same behavior can be observed for the bands due to the carboxylic acid group of candesartan (1705 cm^{-1}, 1426 cm^{-1}, 1212 cm^{-1}, 823 cm^{-1}, and 1260 cm^{-1} (Raman)). These bands weaken their intensity upon salt or complex formation. Besides, the strong Raman band of candesartan located at 1260 cm^{-1} (with COH and NCH bending components) appeared as a weak band in the sodium salt and blue shifted (18 cm^{-1}) with medium intensity in the copper complex. New or more intense bands due to the carboxylate group moiety can be observed in the sodium salt and in the copper complex at ca. 1463 cm^{-1}, 1384 cm^{-1}, 1151 cm^{-1} and 849 cm^{-1}. Besides the bands associated to the antisymmetric stretching mode of the carboxylate group were located at 1647 cm^{-1} (sodium salt) and 1649 cm^{-1} (copper complex), and the bands belonging to the symmetric stretching vibrational mode were located at 1354 cm^{-1} and 1352 cm^{-1}, respectively. The difference between these modes ($\Delta\nu = \nu_{as} - \nu_s$) in the sodium salt is 293 cm^{-1} and in the candesartan copper complex, 297 cm^{-1}, suggesting a monodentate coordination mode [27].

The FTIR assignments for trityl candesartan were performed by comparison with the vibrational modes of candesartan and its sodium salt. The main differences between the two sartans are the typical vibrations due to the presence of the trityl group and the absence of the N–H (protonated tetrazole) modes (see Table 2).

The strong bands observed at 750 cm^{-1} and 700 cm^{-1} are typical for monosubstituted benzenes, (aromatic C–H out of plane) like the trityl group [28]. The bands due to the carboxylic acid group at 1705 cm^{-1}, 1475 cm^{-1}, 1430 cm^{-1}, 1238 cm^{-1}, 1187 cm^{-1} (Raman) and 874 cm^{-1}, shifted or appeared with low intensity both in the sodium salt and in the copper complex. On the other hand, the bands related to the deprotonated product, the carboxylate group, appeared in the sodium salt at 1618 cm^{-1} 1416 cm^{-1}, 1389 cm^{-1}, 1152 cm^{-1} and 1067 cm^{-1} with modifications in the copper complex mainly in the 1445–1420 cm^{-1} region. The difference between antisymmetric and symmetric stretching vibrational modes gives a value of 202 cm^{-1} (sodium salt) and 173 cm^{-1} (copper complex). The lower difference in the value ($\Delta\nu = \nu_{as} - \nu_s$) of the carboxylate stretching modes in the complex is indicative of a bridge $RCOO^-$ coordination to the metal centers [27].

3.2. Electron spin resonance spectra

The X- and Q-band EPR powder spectra of [Cu(Cand)$(H_2O)_4$] (CuCand) was measured at room temperature. The polycrystalline sample in the X-band (Fig. 2) shows a fourline hyperfine splitting pattern due to the coupling of the unpaired electron and the ^{63}Cu nucleus (I = 3/2).

Simulation has shown that the complex exhibits a monomeric type signal with axial symmetry. The calculated Hamiltonian parameters were g = 2.283 ($A = 176\times10^{-4}$ cm^{-1}) and $g_\perp$ = 2.061 ($A_\perp = 15\times10^{-4}$ cm^{-1}). The trend exhibited by the g values ($g > g_\perp$) is consistent with the square bipyramidal Cu(II) complexes with a d_{x2-y2} ground state [29]. The lowest value of g > 2.04 is characteristic of a copper(II) ion in elongated octahedral square-based stereochemistries. The simulated value of the parallel component of the hyperfine coupling constant is similar to that found in copper complexes with chromophores containing N and O donor atoms in the coordination sphere [19,30,31].

Additionally, in an axial symmetry the ratio of g-values, $G = (g - 2)/(g_\perp - 2)$, provides an indication about the magnitude of

Table 2
Assignment of the main bands of the FTIR and Raman spectra of protonated trityl candesartan (HTCand), trityl candesartan sodium salt (NaTCand), and the copper complex (CuTCand) (band positions in cm^{-1}).

Assignment	HTCand		CuTCand		NaTCand	
	FTIR	Raman	FTIR	Raman	FTIR	Raman
υ C=O + δ COH	1705 s	1708 m	1701 w			
υ C=C + υ C=N_{Bz}	1608 m	1603 s	1618 s	1600 s	1618 s	1609 sh
υ_{as} COO^-			1595 m, sh		1578 s	1603 s
δ_{ip} CCH $_{arom}$ + υ C=C + υ *C–$C_{(biph,\ tetrz)}$*	1547 vs	1529 m	1547 vs	1557 vw	1547 vs	1543 vw
δ $_{ip}$ CCH $_{arom}$ + scissor CH_2 + def CH_3 + ***υ C–C $_{tz\text{-}biph}$***	1519 vw	1519 sh	1510 vw	1528 w	1516 vw	1526 w
						1511 w
υ C–C $_{tz\text{-}biph}$ + δ_{ip} CCH $_{arom}$	1481 sh	1493 m	1491 m		1484 m	
δ CCH ip + scissor CH_2 + **δ COH** + υ CN_{Bz}	1475 s 1439 s, sh	1467 m 1461 m	1463 m		1463 m	1461 w
					1457 sh	
			1445 s	1449 m	1416 m	1423 w
υ C=N $_{Bz,\ tz}$ + δ_{ip}CCH_{Bz} + ω CH_2 + τ CH_2 + **δ COH + υ_s COO^-**	1430 s	1430 w	1427 m	1405 m	1405 sh	1411 w
			1412 w			
δs CH_3 + ω CH_2 + υ CN_{Bz} + ***υ C-COO^-***	1388 m	1360 w	1389 s	1378 w	1389 s	1391 vw
ω CH_2 + υ C=C + υ CN_{Bz}	1353 m	1359 w	1353 m	1334 sh	1354 m	
				1316 w	1313 w	
τ CH_2 + δ CCH + δ NCH + υ CN_{Bz}	1284 m	1297 m	1277 m	1282 w	1278 m	1296 m
		1285 sh				1280 m
δ COH + υ NN	1238 vs	1257 m	1255 w	1257 m	1259 sh	1245 m
		1226 m				1226 w
***υ* CO (COH)**	1216 sh	1187 m	1220 w	1210 w		1202 vw
+ υ NN + δ CCH_{arom}	1196 sh		1208 sh			1185 w
$\delta_{ip\ arom}$ CCH + ρ CH_2 + ω CH_2 +	1153 sh 1136 m 1112 sh	1150 m	1153 m	1160 w	1152 m	1160 m
υ CN_{Bz} + ***υ (Bz)C–C(COO^-)***		1139 w 1119 w	1115 w	1134 w	1112 w	1153 sh
δ NNN + δ NCN + δ_{op} CCH + ***υ (Bz)C–C(COO^-)***	1072 sh	1004 s	1068 m	1003 s	1067 m	1002 vs
	1038 s		1038 s 1008 m		1040 s	
	1005 m				1009 m	
δ_{op} COH + δ_{op} CCH_{Bz} + δ CCC (Et) + ***π CCOO (COO^-)***	874 m	814 s	872 w	813 w	874 w	814 w
	840 w		849 vw		818 w	
	813 w		820 w			
δ_{op} CH (trityl) + δ_{op} CCH + $\delta_{ip}$$CCC_{arom}$	750 vs	740 w	748 sh 760 vs	780 w	785 sh	787 w
					755 s	750 vw
δ_{op} CH (trityl) + **δ OCO (COOH)** + δ (Bz)COC (Et)	700 s		700 vs	700 w	701 vs	700 w
Biph breath	675 sh	668 w	670 sh	656 w	670 sh	667 vw

Bold: main modes of HTCand. Bold *italics*: main modes of NaTCand and CuTCand.
Abbreviations: see Table 1 footnote.

the exchange interactions between the copper centers in the polycrystalline solid. According to Hathaway [29] a G value less than four indicates a considerable exchange interaction in the solid complexes, while a higher value indicates that the magnetic interaction is negligible. In complex **[1]**, G is 4.64 which indicates the occurrence of no interaction between the copper centers.

For the dinuclear complex, $[Cu_2(TCand)_4(H_2O)_2]\cdot 4H_2O$ (CuTCand), the observed broadening of the resonance line centered at c.a. 3200 Gauss indicates the presence of an antiferromagnetic spin-spin interaction (Fig. 3, solid line) [32,33]. The nature of the exchange coupling within Cu–Cu pairs is evident from the thermal dependence of EPR spectrum intensity (Fig. 3, dotted line). While temperature decreases, the triplet state becomes depopulated and in consequence the spectrum drops intensity. At 5 K (Fig. 3, dotted line) a weaker signal corresponding to the presence of a small amount of monomeric impurity is observed. This signal is usually found in dinuclear copper carboxylate complexes [34].

These results are in agreement with the data obtained from the diffuse reflectance spectra. The presence of interactions between the metal centers in **[2]** is consistent with the typical shoulder that appears at

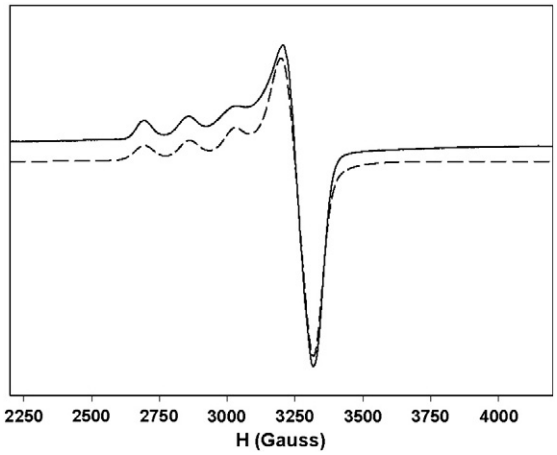

Fig. 2. EPR powder spectra (X-band) of the $[Cu(Cand)(H_2O)_4]$ (CuCand) complex at 300 K (solid line) and its simulated spectrum (WINEPR SimFonia) (dotted line).

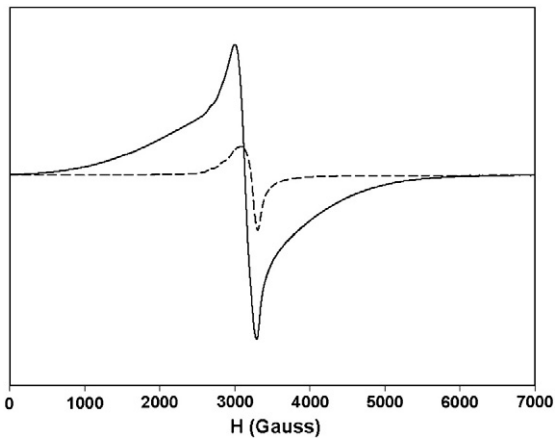

Fig. 3. EPR powder spectra (X-band) of the $[Cu_2(TCand)_4(H_2O)_2]\cdot 4H_2O$ (CuTCand) complex at 300 K (solid line) and 5 K (dotted line).

around 400 nm [19,26]. In particular, the trityl candesartan–copper dimeric complex showed a spectral pattern similar to that of valsartan–copper (380 nm–750 nm). The coordination spheres of both metal complexes are composed by oxygen atoms from bridging carboxylates and water acting as ligands.

The new chelates are insoluble in water and are very soluble in ethanol, DMSO and dimethylformamide (DMF). The analytical data C, H, N and the thermal analysis confirm the composition of the complexes and the stoichiometry proposed. Evidence of the mode of bonding of the ligands was gathered from the IR and Raman spectra, while their geometry was assumed from the electronic and EPR spectra. The proposed structures are shown in Fig. 4. Unfortunately, the different assays performed to obtain single well-ordered crystals in order to solve their crystal structure failed in both cases.

3.3. Spectrophotometric and stability determinations

The spectrophotometric titration of candesartan:Cu (Fig. 5) was measured using different ligand-to-metal molar ratios in ethanolic solutions from L:M 10 to 0.75 at pH 8.4. A 1:1 (L:M) final stoichiometry was determined in agreement to the structural determination of the solid complex.

Additionally, a final 2:1 (L:M) stoichiometry for the trityl candesartan–copper complex was determined under the same experimental conditions and pH 7 (Fig. 6).

The UV–vis spectrum of **[1]** (670 nm, ethanolic solution, pH 8.4) was different from the diffuse reflectance spectrum measured for the solid compound, indicating a probable replacement of the coordinated water molecules by ethanol. The formation of **[1]** was followed spectrophotometrically at the pH value used in its synthesis. The visible spectra of ethanolic 1:1 solutions of candesartan and copper(II) (0.025 M) at different pH values were measured (Fig. 7). At low pH values, the spectral pattern corresponded to that of an ethanolic solution of $CuCl_2 \cdot 2H_2O$. In the range of pH values 6<pH<9 the bands displayed at 670 nm indicated complex formation. Then, at higher pH values, turbidity was observed probably arising to copper(II) hydroxides or alkoxides formation.

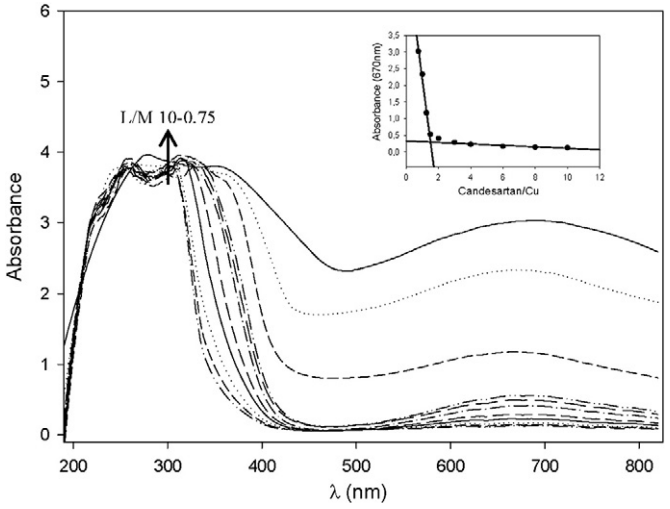

Fig. 5. UV–vis spectra of candesartan (0.01 M) with the addition of $CuCl_2 \cdot 2H_2O$ in ligand-to-metal ratios (L/M) from 10.0 to 0.75 (pH 8.4) in ethanol. The arrow indicates increased metal additions. Inset: spectrophotometric determinations of CuCand complex stoichiometry at 670 nm by the molar ratio method.

On the other hand, the stability of the complex was assessed following the changes of the electronic spectral band of **[1]** as a function of time (ethanolic solution, 5×10^{-3} M). Since the absorbance of the solution was reduced ca. 3% in 60 min it was determined that the complex is stable at least under these experimental conditions, allowing the determination of the antioxidant and antihypertensive properties in this solvent. Besides, the EPR solution spectrum (DMSO) afforded monomeric type signal (not shown) with a g_{iso} value of 2.13

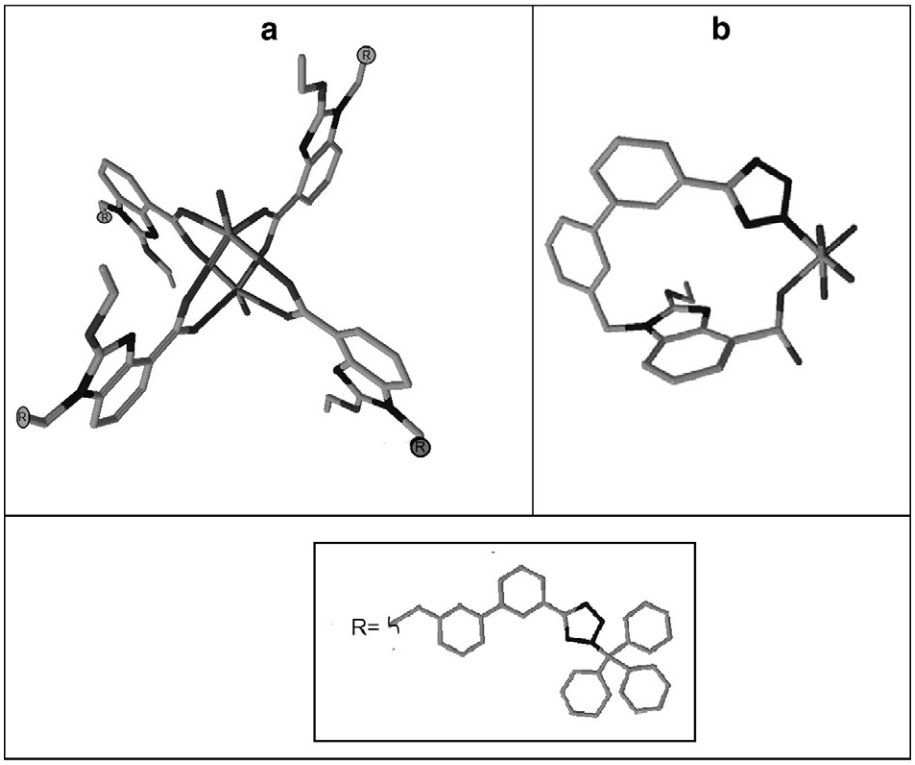

Fig. 4. Proposed structures of $[Cu_2(TCand)_4(H_2O)_2] \cdot 4H_2O$ (a) and $[Cu(Cand)(H_2O)_4]$ (b).

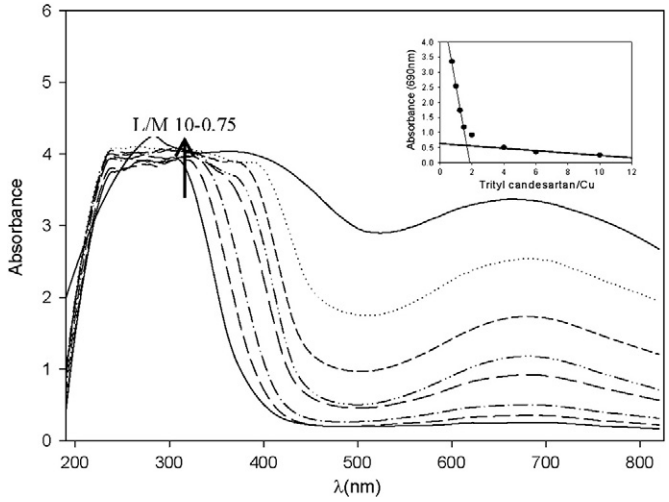

Fig. 6. UV–vis spectra of trityl candesartan (0.015 M) with the addition of $CuCl_2 \cdot 2H_2O$ in ligand-to-metal ratios (L/M) from 10.0 to 0.75 (pH 7) in ethanol. The arrow indicates increased metal additions. Inset: spectrophotometric determinations of CuTCand complex stoichiometry at 690 nm by the molar ratio method.

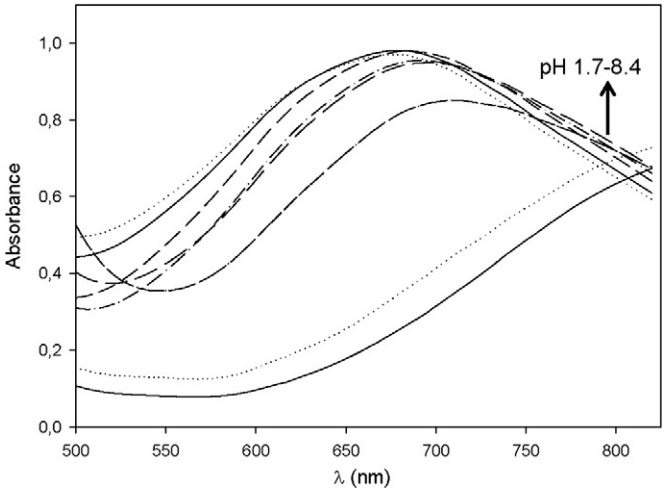

Fig. 8. Spectrophotometric determination of the formation of the CuTCand complex formation in solution. Visible spectra of ethanolic 2:1 solutions of trityl candesartan and copper (0.025 M:0.0125 M) at different pH values.

which is very close to the value calculated for the solid complex suggesting that the square bipyramidal structure is retained after dissolution.

The spectral changes of ethanolic 2:1 solutions of 0.025 M:0.0125 M trityl candesartan:copper(II) at different pH values are shown in Fig. 8.

It can be seen that the formation of the complex occurred at pH values between 4 and 8 and at higher pH values turbidity was observed probably due to copper(II) hydroxide or alkoxide formation.

The stability of the solid complex **[2]** in ethanolic and DMSO solutions (4×10^{-3} M) was monitored in the time period of 0–60 min, and it was observed that the complex is stable for at least 1 h (the intensity of the bands remained unchanged). The UV–vis solution spectra of **[2]** in ethanol and DMSO solvents are closely similar showing a slight red shift of ca. 10 nm for the ethanolic solutions due to solvatochromic effects. The presence of the band located at 400 nm in both spectra which was also identified in the reflectance spectrum of the solid complex could be indicative of the retention of the dimeric structure in solution (carboxylate bridge, see FTIR section). The EPR spectra of both solutions showed a very poor resolved signal. The formation of substantial proportions of monomeric complex (breakage of the carboxylate bridge) was discarded because of the absence of the monomeric signals suggesting that the complex preserves its dinuclear composition after dissolution.

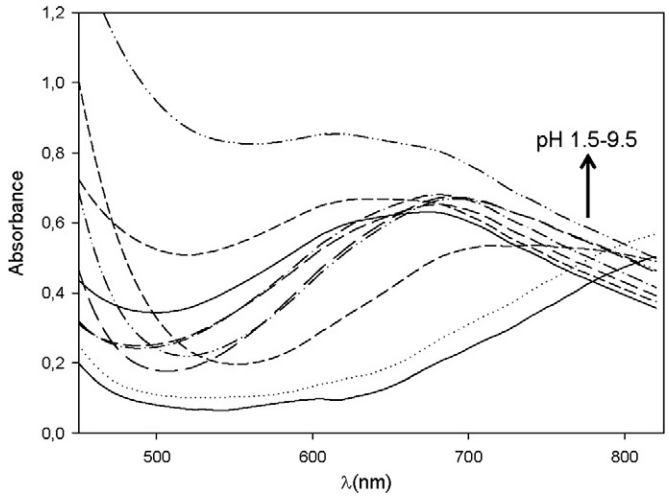

Fig. 7. Spectrophotometric determination of the CuCand complex formation in solution. Visible spectra of ethanolic 1:1 solutions of candesartan and copper (0.025 M) at different pH values.

3.4. Antioxidant activities

Biological free radical reactions generally involve molecular oxygen reduction ultimately yielding reactive oxygen species (ROS), including superoxide anion and peroxyl radical. ROS are recognized as harmful agents causing strong injuries to several cell components such as lipids, proteins and DNA, which are gradually damaged [35]. The oxidative injuries caused by ROS are actually acknowledged as active contributors to aging and degenerative diseases, such as brain dysfunction, i.e., Parkinson's and Alzheimer's syndromes, cardiovascular disorders and cancer. Oxygen stress is associated with hypertension but it seemed that ROS production is a consequence of the vascular damage produced in hypertensive patients [36]. Therefore, the antioxidant activity of the different compounds could be a contributory factor to the antihypertensive effects. So, the ability of the ligands and the complexes to act as free radical scavengers was tested.

The assay for the total antioxidant activity measures the concentration of an antioxidant compound that suppresses the absorbance of $ABTS^{\cdot+}$ at 734 nm (basal conditions). The total antioxidant activity values obtained for both sartans and their copper(II) complexes were similar (Fig. 9), and showed that these compounds were not able to scavenge the ABTS radical cation. The low capacity of suppressing the radical cation of ABTS was also determined by the TEAC (total equivalent antioxidant coefficient) values that ranged between 0.01 and 0.03, considering a value of 1 for Trolox.

The same loss of antioxidant capacity was found in the study of the scavenging power of the DPPH radical (Fig. 10). A total basal inhibition of the radical DPPH at 500 μM of 6% was found for complex **[2]**.

Pyranine is a spectrometric probe that scavenges free radicals, including $ROO^{\bullet}$ radicals. The decrease in pyranine intensity at 454 nm was followed to monitor the decay of the absorbance curve to determine the antioxidant activities against peroxyl radicals. Peroxyl radicals were generated by the thermal decomposition of AAPH (2,2-azobis(2-amidinopropane) dihydrochloride) [37] and this substance can generate free radicals at a steady rate for extended periods of time (half life of 175 h). The consumption of pyranine was followed spectrophotometrically with a thermostated cell at 37 °C by the decrease in absorbance at 454 nm. The reaction solutions

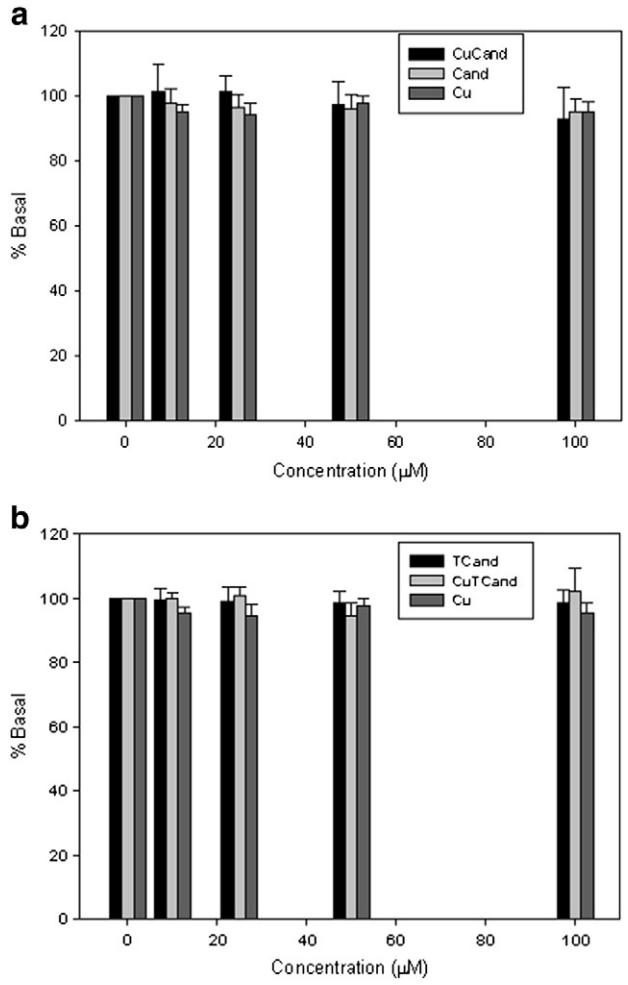

Fig. 9. Total antioxidant activity measured as the reduction of the concentration of the radical cation of 2,2′-azino-bis(3-ethyl-benzothiazoline-6-sulfonic acid diammonium salt) ($ABTS^{\cdot+}$) by the addition of a) candesartan, CuCand and $CuCl_2.2H_2O$ and b) trityl candesartan, CuTCand and $CuCl_2 \cdot 2H_2O$. The values are expressed as the mean ± standard error of at least three independent experiments.

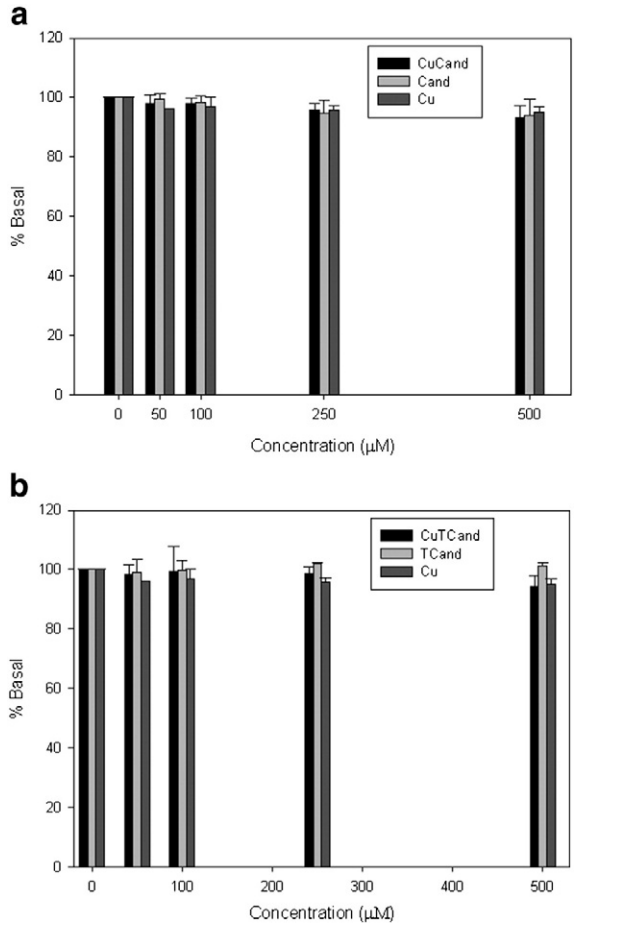

Fig. 10. Scavenge of 1,1-diphenyl-2-picrylhydrazyl radical (DPPH) by a) candesartan, CuCand and $CuCl_2 \cdot 2H_2O$ and b) trityl candesartan, CuTCand and $CuCl_2 \cdot 2H_2O$. The values are expressed as the mean ± standard error of at least three independent experiments.

contained AAPH (50 mM), pyranine (50 μM) and several concentrations of the tested compounds. The delay of pyranine consumption (lag phase) was calculated as the time due to the consumption of peroxyl radicals, before the consumption of pyranine (notable reductions in absorbance) [31]. Both experimental data, the area under the curve or the lag phase can be used to determine the capacity of a substance to scavenge peroxyl radicals. An appreciable lag phase for complex **[2]** in a dose response manner was observed (Fig. 11a), but no lag phase has been obtained for **[1]** (Fig. 12). Besides, complex **[2]** exhibited a good peroxyl radical scavenging capacity in contrast with the two sartans and $CuCl_2 \cdot 2H_2O$ (data not shown). In Fig. 11b the comparison of the ability to scavenge $ROO^{\cdot}$ radicals with a potent antioxidant, trolox, has been performed. As is expected, trolox behaved as a better anti peroxyl radical agent than complex **[2]**. The slopes of the curves of induction time versus concentration (Fig. 11b) indicated an improvement of the reactivity of trityl candesartan towards the peroxyl radicals by complexation with copper (experimental slopes: 0.358, 0.143, and 0.00486 for trolox, **[2]**, and trityl candesartan, respectively). At concentrations of 100 μM the calculated lag phases are: 35.94 min, 15.209 min and 3.504 for trolox, complex **[2]** and trityl candesartan, respectively.

Several Cu(II) compounds containing small bioligands were able to mimic SOD activity by scavenging the superoxide ion. The superoxide scavenging assay was based on a nonenzymatic method at pH = 7.4. In this test, the superoxide anion radicals were generated by the reaction of NADH with PMS, and detected through the reduction of NBT. The SOD activity had been defined as the concentration of the tested compounds for the 50% inhibition of the NBT reduction by superoxide produced in the system (IC_{50} values) and was evaluated from the absorbance decrease at 560 nm compared to the blank (the reaction mixture without the addition of the different compounds). Under our experimental conditions the sartans did not show any scavenging capacity. The IC_{50} value measured for $CuCl_2 \cdot 2H_2O$ (3.2×10^{-6} M) was very low. This behavior was also shown by other authors using another copper(II) salts and they stated that these ions produced a high SOD mimetic behavior [38,39]. However, Huber et al. pointed out that copper(II) ions could also oxidize the reduction product of NBT, so the high SOD activity found for copper(II) ions may be due to reactions occurring between the ions and the formazan during the experimental determinations [40]. Therefore, it is not recommended to apply this technique to copper(II) salts. In Fig. 13, it can be seen that the poor antioxidant capacities of the sartans were improved by complexation (IC_{50} **[1]** $= 6.8 \times 10^{-6}$ M and IC_{50} **[2]** $= 3.7 \times 10^{-6}$ M). The prepared mimetic complexes were not as effective as the enzyme (bovine erythrocyte SOD, $IC_{50} = 2.1 \times 10^{-7}$ M) [41] but it has been previously determined that when the experimental IC_{50} values occurred below 20×10^{-6} M the compounds are considered to act as strong SOD mimics [42].

The IC_{50} values are not appropriate for making direct comparisons with literature data because of the different methods employed in each experience. The kinetic constant values of the reactions (k) which are independent of the nature and concentration of the detector can then be calculated. Taking into account that at the IC_{50} values

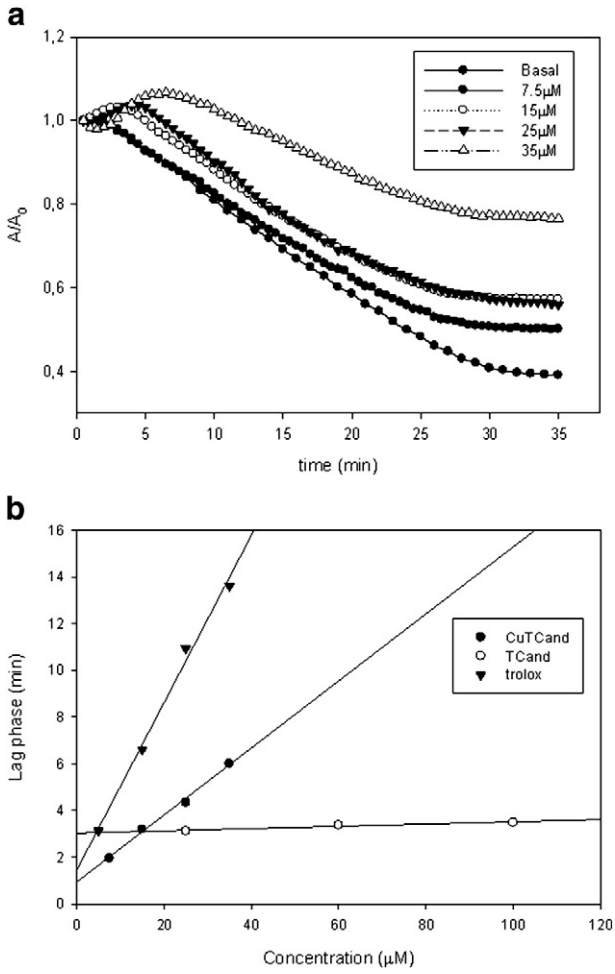

Fig. 11. a) Scavenge of peroxyl radicals measured as the decay of the intensity of pyranine by addition of different concentrations of CuTCand (A_o, initial intensity, 454 nm); b) Effect of trityl candesartan, CuTCand and Trolox on AAPH-generated peroxyl radicals and pyranine mixture. Changes on time delay (lag phase) upon the different concentrations of added substances.

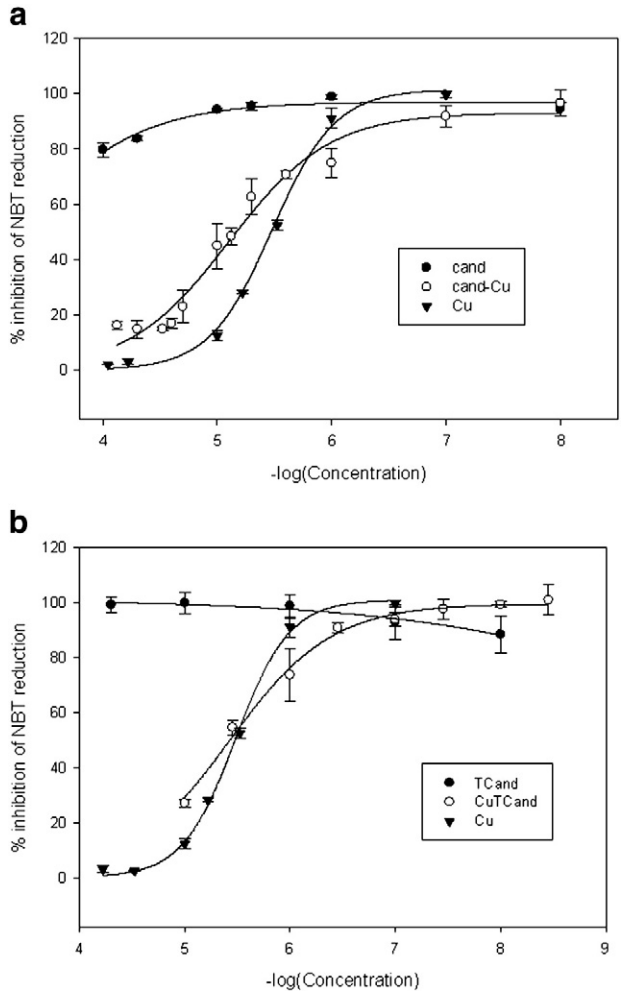

Fig. 13. Effect of a) candesartan, CuCand and $CuCl_2.2H_2O$ and b) trityl candesartan, CuTCand and $CuCl_2 \cdot 2H_2O$ on the reduction of nitroblue tetrazolium by nonenzymatically generated superoxide (phenazine methosulfate and reduced nicotinamide adenine dinucleotide system).

superoxide reacts at the same speed with the detector and the tested substances, $k = k_{detector} \cdot [detector]/IC_{50}$. Considering k_{NBT} (pH = 7.8) = 5.94×10^4 M^{-1} s^{-1} [43] the different constants were determined (see Table 3).

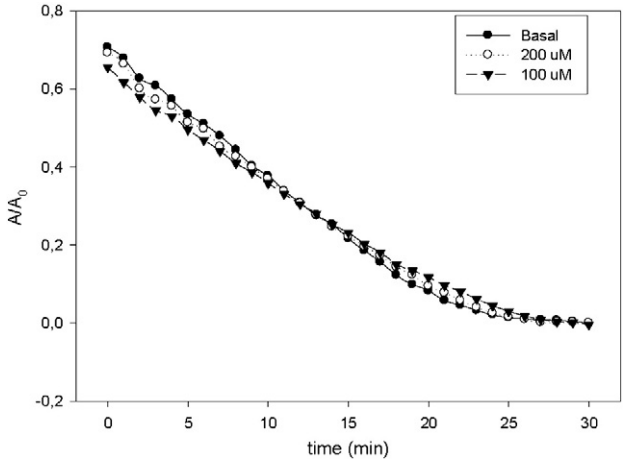

Fig. 12. Effect of CuCand on AAPH-generated peroxyl radicals and pyranine mixture. A/A_o, experimental absorbance/zero time absorbance at 454 nm.

From these experimental values the good SOD-like activities of the copper complexes was established. In conclusion, the two new copper complexes exert antioxidant effects against peroxyl radicals in the case of complex **[2]** and superoxide anion for both complexes.

3.5. Reduction of surface area in human mesangial cells

The ability of angiotensin II to reduce the PCSA in HMC pre-treated with sartans and their copper complexes is analyzed. Human mesangial cells express angiotensin II receptors and showed contractile response in the presence of this peptide. Changes in PCSA are considered to be a consequence of cell contraction, and are due to the interaction of angiotensin II with its receptor [44]. Our results presented in Fig. 14 and

Table 3
IC_{50} values and kinetic constants of candesartan, trityl candesartan, their copper complexes, $CuCl_2$ and bovine erythrocyte superoxide dismutase.

Compound	IC_{50} (μM)	k (M^{-1} s^{-1})
Cand	[a]	[a]
CuCand	6.8	2.6×10^6
TCand	[a]	[a]
CuTCand	3.7	4.8×10^6
$CuCl_2$	3.2	5.6×10^6
SOD	0.2	8.9×10^7

[a] Inactive.

Table 4 provide evidence that both complexes inhibited the angiotensin II-induced PCSA reduction. The PCSA ranged between 97% with CuTCand and 100.8% with CuCand.

Statistically significant differences were not observed in the inhibition of the contraction when very low concentrations (10^{-8} M) of copper(II) and the ligands individually were tested. This behavior is similar to that found in combined therapies adding candesartan to ACE (angiotensin-converting-enzyme) inhibitors such as enalapril. In these clinical trials no effect on oxidative stress and no improvement of endothelial function or exercise capacity in patients with chronic heart failure were found [45]. Besides, it was also demonstrated that candesartan is able to suppress fatty acid induced oxidative stress in pancreatic β-cells but it remained unclear whether sartans served as scavengers against oxidative stress [10].

Preliminary data suggest that oxidative stress which is mainly mediated by superoxide is a primary or secondary cause of many chronic diseases including hypertension, because they contribute to the narrowing of arterial lumen with the consequent increase in peripheral resistance and blood pressure [46]. Antioxidant vitamins may improve vascular damage and reduce blood pressure in patients with essential hypertension. In a previous paper it was demonstrated that losartan has protection against oxidative stress in hypertensive patients [47]. In this paper it has been demonstrated that the lack of antioxidant effects of both sartans was improved by complexation. The increase of the superoxide scavenging activity upon complexation may be the reason of the higher expansive activity on the surface area of HMC. On the other hand, it has been assumed that candesartan induces conformational changes at the AT1 receptor that prevent agonist binding. Another hypothesis takes into account the tight binding and the slow dissociation of the sartan that causes a prolonged functional loss of the occluded receptors [48]. In a previous study candesartan was docked into the AT1 receptor and its interaction with Phe 171, Phe 182, Tyr 184, Lys 199 and His 256 residues of AT1receptor model was demonstrated [49]. Besides, the anionic tetrazole ring did not appear to interact with any residue. The interaction of the carboxylate and tetrazolate moieties of the sartan with copper(II) may induce new conformational changes probably fitting most with the binding pocket of AT1 receptor. It can then be seen that the complexation probably enhances the properties as angiotensin II receptor blockers.

Table 4
Percentage of the planar cell surface area. CT, basal conditions. AT2, addition of angiotensin II (10^{-6} M) after a previous incubation of the cells with each compound (10^{-8} M) during 15 min.

Compound	% PCSA (mean ± SEM)
CT	99.75 ± 0.03
AT2	80.75 ± 2.15
CuTCand	96.50 ± 2.65
TCand	87.05 ± 1.07
CuCand	100.40 ± 0.50
Cand	86.35 ± 1.21
$CuCl_2$	87.90 ± 0.04

4. Conclusions

Two new copper complexes with sartans were synthesized and characterized. Copper(II) forms a mononuclear complex with candesartan **[1]** and a dinuclear complex with carboxylate bridges with its tritylated compound **[2]**. The dissolutions of both compounds in DMSO and ethanol confirm that they retain their structures and are stable at least during 60 min. At the tested concentrations both sartans do not show antioxidant activities and do not produce expansion of the previously contracted cells. It was proved that the copper complexes acted as good superoxidedismutase simil agents and as a result they produced an improvement of the inhibition of the angiotensin II-induced contraction of the human mesangial cells. In conclusion, the complexes exhibit even higher efficiency as drugs in comparison with the free non-complexed medication, showing antioxidant abilities and expressing higher effect in the ability to block the angiotensin II receptor.

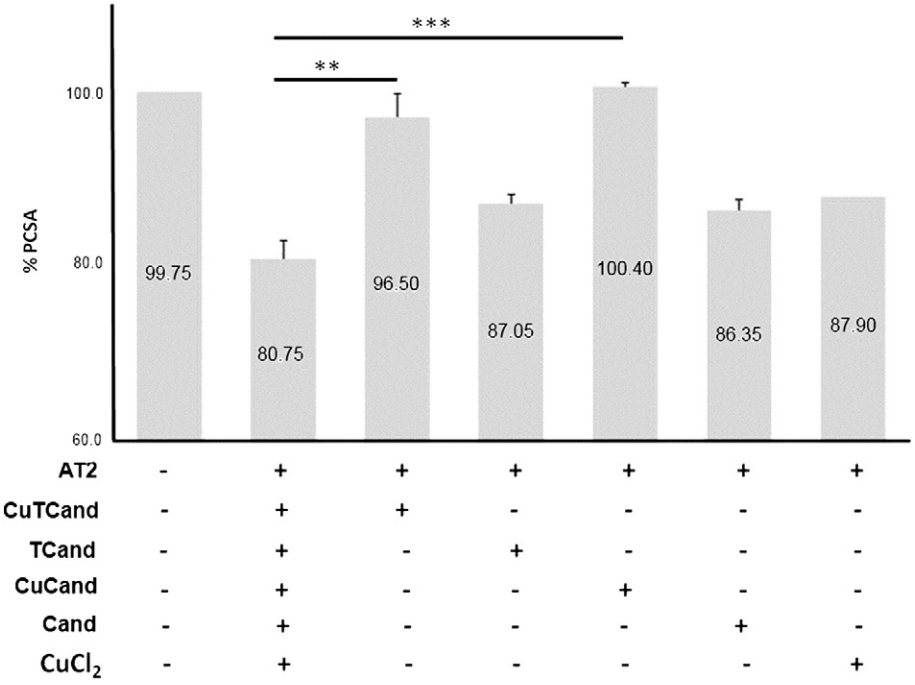

Fig. 14. HMC were incubated with 10^{-8} M trityl candesartan (HTCand), candesartan (H_2Cand) or their copper(II) complexes (CuTCand and CuCand, respectively). After 15 min, the cells were incubated with 10^{-6} M Angiotensin II (AT2) for 30 min. The changes in PCSA were determined by computerized planimetric techniques. The results are expressed as a percentage of basal planar cell surface at 30 min with Angiotensin II (100% is the value obtained at 0 min). The mean ± SEM of three different experiments are shown. ** $p<0.01$ cells treated with CuTCand plus AT2 *vs.* AT2, ***$p<0.001$ cells treated with CuCand plus AT2 *vs.* AT2.

Abbreviations

AAPH	2,2-azobis(2-amidinopropane) dihydrochloride
ABTS	2,2′-azino-bis(3-ethyl-benzothiazoline-6-sulfonic acid diammonium salt)
ACE	Angiotensin converting enzyme
AT2	Angiotensin II
DHR123	Dihydrorhodamine 123
DMEM	Dulbecco's Modified Eagle's Medium
DMF	N,N-dimethylformamide
$DPPH^{\cdot}$	1,1-diphenyl-2-picrylhydrazyl radical
DTA	Differential thermal analysis
HMC	Human mesangial cells
NADH	Nicotinamide adenine dinucleotide
NBT	Nitroblue tetrazolium
PCSA	Planar cell surface area
PMS	Phenazine methosulfate
RAS	Renin–angiotensin system
ROS	Reactive oxygen species
SOD	Superoxidedismutase
TEAC	Trolox equivalent antioxidant coefficient
TGA	Thermogravimetric analysis
Trolox	6-hydroxy-2,5,7,8-tetramethylchroman-2-carboxylic acid

Acknowledgements

This work was supported by UNLP, CONICET (PIP1125), ANPCyT (PICT 2008-2218), SAF2010-16198 and CICPBA. EGF is a member of the Carrera del Investigador, CONICET. PAMW is a member of the Carrera del Investigador CICPBA, Argentina. MSI is a fellowship holder from CONICET.

References

[1] J.L. León Alvarez, New Therapeutics in Hypertension, in: H. Babaei (Ed.), Antihypertensive drugs, InTech, Croatia, 2012, (Chapter 1).
[2] C.H. Gleiter, C. Jägle, U. Gresser, K. Mörike, Cardiovasc. Drug Rev. 22 (2004) 263–284.
[3] T. Unger, Eur. Heart J. Suppl. 6 (2004) H11–H16.
[4] D. Herr, M. Rodewald, G. Hack, R. Konrad, R. Kreienberg, C. Wulff, J. Clin. Oncol, 2007 ASCO Annual Meeting Proceedings Part I, vol. 25, No. 18S, 2007, p. 14114, (June 20 Supplement).
[5] M. Kosugi, A. Miyajima, E. Kikuchi, Y. Horiguchi, M. Murai, Clin. Cancer Res. 12 (2006) 2888–2893.
[6] A. Miyajima, T. Kosaka, T. Asano, K. Seta, T. Kawai, M. Hayakawa, Cancer Res. 62 (2002) 4176–4179.
[7] Y. Fujimoto, T. Sasaki, A. Tsuchida, K. Chayama, FEBS Lett. 495 (2001) 197–200.
[8] H. Yoshiji, S. Kuriyama, H. Fukui, Tumor Biol. 23 (2002) 348–356.
[9] K.P.S. Adinarayana, P. Ajay Babu, R. Karuna Devi, J. Pharm. Res. Rev. 2 (2012) 24–27.
[10] Y. Saitoh, W. Hongwei, H. Ueno, M. Mizuta, M. Nakazato, Diabetes Res. Clin. Pract. 90 (2010) 54–59.
[11] S. Chen, Y. Ge, J. Si, A. Rifai, L.D. Dworkin, R. Gong, Kidney Int. 74 (2008) 1128–1138.
[12] P.R. Andrews, D.J. Craik, J.L. Martín, J. Med. Chem. 27 (1984) 1648–1657.
[13] G. García, M. Rodríguez-Puyol, R. Alajarín, I. Serrano, P. Sánchez-Alonso, M. Griera, J.J. Vaquero, D. Rodríguez-Puyol, J. Álvarez-Builla, M.L. Díez-Marqués, J. Med. Chem. 52 (2009) 7220–7227.
[14] M.C. Breschi, V. Calderone, M. Digiacomo, A. Martelli, E. Martinotti, F. Minutolo, S. Rapposelli, A. Balsamo, J. Med. Chem. 47 (2004) 5597–5600.
[15] M.C. Breschi, V. Calderone, M. Digiacomo, M. Macchia, A. Martelli, E. Martinotti, F. Minutolo, S. Rapposelli, A. Rossello, L. Testai, A. Balsamo, J. Med. Chem. 49 (2006) 2628–2639.
[16] S. Inutsuka, S. Araki, Cancer 42 (1978) 626–631.
[17] L.M. Klevay, Ann. N. Y. Acad. Sci. 355 (1980) 140–151.
[18] S.B. Etcheverry, E.G. Ferrer, L. Naso, D.A. Barrio, L. Lezama, T. Rojo, P.A.M. Williams, Bioorg. Med. Chem. 15 (2007) 6418–6424.
[19] S.B. Etcheverry, A.L. Di Virgilio, O.R. Nascimento, P.A.M. Williams, J. Inorg. Biochem. 107 (2012) 25–33.
[20] WINEPR SimFonia, vol. 25, Bruker Analytische Messtecnik GmbH, 1996.
[21] T. Yamaguchi, H. Takamura, T.C. Matoba, J. Terao, Biosci. Biotechnol. Biochem. 62 (1998) 1201–1204.
[22] R. Re, N. Pellegrini, A. Proteggente, A. Pannala, M. Yang, C. Rice-Evans, Free Radic. Biol. Med. 26 (1999) 1231–1237.
[23] S. Gorinstein, S. Moncheva, E. Katrich, F. Toledo, P. Arancibia, I. Goshev, S. Trakhtenberg, Mar. Pollut. Bull. 46 (2003) 1317–1325.
[24] C.D. Hapner, P. Deuster, Y. Chen, Chem. Biol. Interact. 186 (2010) 275–279.
[25] C.C. Kuo, M. Shih, Y. Kuo, W. Chiang, J. Agric. Food Chem. 49 (2001) 1564–1570.
[26] M.S. Islas, C.A. Franca, S.B. Etcheverry, E.G. Ferrer, P.A.M. Williams, Vibrat. Spectrosc. 62 (2012) 143–151.
[27] K. Nakamoto, Infrared and Raman Spectra of Inorganic and Coordination Compounds, Part B, 5th ed., Wiley, New York, 1997.
[28] F.S. Parker, Applications of Infrared, Raman, and Resonance Raman Spectroscopy in Biochemistry, Plenum Press, New York, 1983.
[29] B.J. Hathaway, D.E. Billing, Coord. Chem. Rev. 5 (1970) 143–207.
[30] T. Kohzuma, A. Odani, Y. Morita, M. Takani, O. Yamauchi, Inorg. Chem. 27 (1988) 3854–3858.
[31] Y. Mino, T. Ishida, N. Ota, M. Inoue, K. Nomoto, H. Yoshioka, T. Takemoto, Y. Sugiura, H. Tanaka, Inorg. Chem. 20 (1981) 3440–3444.
[32] H. Ohtsu, Y. Shimazaki, A. Odani, O. Yamauchi, W. Mori, S. Itoh, S. Fukuuzumi, J. Am. Chem. Soc. 122 (2000) 5733–5741.
[33] K. Ösz, K. Várnagy, H. Süli-Vargha, A. Csámpay, D. Sanna, G. Micera, I. Sóvágó, J. Inorg. Biochem. 98 (2004) 1655–1666.
[34] D. Kovala-Demertzi, D. Skrzypek, B. Szymanska, A. Galani, M.A. Demertzis, Inorg. Chim. Acta 358 (2005) 186–190.
[35] E.G. Ferrer, P.A.M. Williams, Modification of flavonoid structure by oxovanadium(IV) complexation, in: K. Yamane, Y. Kato (Eds.), Biological effects, Handbook on flavonoids: Dietary Sources, Properties and Health BenefitsNova Science Publishers, Inc., New York, 2011, pp. 145–190, (Cap III).
[36] E. Grossman, Diabetes Care 31 (2008) S185–S189.
[37] W.Y. Huang, K. Majumder, J. Wu, Food Chem. 123 (2010) 635–641.
[38] U. Weser, K.H. Sellinger, E. Lengfelder, W. Werner, J. Strahle, Biochim. Biophys. Acta 631 (1980) 232–245.
[39] E. Bienvenue, S. Choua, M.A. Lobo-Rdio, C. Marzin, P. Pacheco, P. Seta, G. Tarrago, J. Inorg. Biochem. 57 (1995) 157–168.
[40] K.R. Huber, R. Scridhar, E.H. Griffith, E.L. Amma, J. Roberts, Biochim. Biophys. Acta 915 (1987) 267–276.
[41] E.G. Ferrer, N. Baeza, L.G. Naso, E.E. Castellano, O.E. Piro, P.A.M. Williams, J. Trace Elem. Med. Biol. 24 (2010) 20–26.
[42] N.A. Roberts, P.A. Robinson, Br. J. Rheumatol. 24 (1985) 128–136.
[43] S. Durot, C. Policar, F. Cisnetti, J.P. Renault, G. Pelosi, G. Blain, H. Korri-Youssoufi, J.P. Mahy, Eur. J. Inorg. Chem. (2005) 3513–3523.
[44] G. Torrecillas, M.C. Boyano-Adanez, J. Medina, T. Parra, M. Griera, S. Lopez-Ongil, E. Arilla, M. Rodriguez-Puyol, D. Rodriguez-Puyol, Mol. Pharmacol. 59 (2001) 104–112.
[45] G.R. Ellis, A.F. Nightingale, D.J. Blackman, R.A. Anderson, C. Mumford, G. Timmins, D. Lang, S.K. Jackson, M.D. Penney, M.J. Lewis, M.P. Frenneaux, J. Morris-Thurgood, Eur. J. Heart Fail. 4 (2002) 193–199.
[46] R.M. Touyz, Curr. Hypertens. Rep. 2 (2000) 98–105.
[47] V. Uday Kiran, N. Venkat Rajaiah, D. Rama Krishna, Y. Narsimha Reddy, Int. J. Pharmacol. 6 (2010) 916–920.
[48] T. Tuccinardi, V. Calderone, S. Rapposelli, A. Martinelli, J. Med. Chem. 49 (2006) 4305–4316.
[49] K. Ohno, Y. Amano, H. Kakuta, T. Niimi, S. Takakura, M. Orita, K. Miyata, H. Sakashita, M. Takeuchi, Ii Komuro, J. Higaki, M. Horiuchi, S. Kim-Mitsuyama, Y. Mori, R. Morishita, S. Yamagishi, Biochem. Biophys. Res. Commun. 404 (2011) 434–437.